ELSEVIER

Journal of Luminescence 76&77 (1998) 441–446

JOURNAL OF LUMINESCENCE

Excited state dynamics in sensitized photon avalanche processes

V. Lupei[a,*], E. Osiac[a], T. Sandrock[b], E. Heumann[b], G. Huber[b]

[a] *Institute of Atomic Physics, 76900 Bucharest, Romania*

[b] *Universität Hamburg, Institut für Laser-Physik, 20355 Hamburg, Germany*

Abstract

The excited state dynamics in photon avalanche processes is discussed on the basis of rate equation modelling for the case of sensitized avalanche. It is thus shown that a cw pump in these systems induces a very complex dynamics of excitation in both the active and sensitized ions. The results are compared with experimental data on avalanche emission of Pr^{3+} in Yb^{3+}-sensitized $YLiF_4$ crystals. It is shown that in real systems the actual distribution of pump intensity at each point of the sample must be taken into account.

Keywords: Photon avalanche; Sensitized avalanche; Pr, Yb:YAG

1. Introduction

Photon avalanche is a strongly non-linear process of population of an emitting high energy level of an active ion under the action of a cw excited state absorption (ESA) from an intermediate level (reservoir), which is populated by a cross-relaxation process whose initial states are the emitting levels and the ground level and the final states both correspond to the reservoir level. If the cross-relaxation process is strong, it could induce an overall quantum efficiency of population of the reservoir larger than unity for each ESA act. Then if the ESA rate is strong enough to overcome other processes of de-excitation of the reservoir level, an avalanche process of population of the reservoir and of the emitting level takes place. Thus the photon avalanche is a threshold process concerning both the efficiency of the cross-relaxation and the ESA pump rate. Although discovered in 1979 [1] the avalanche process attracted increased attention only in the last few years, in connection with construction of upconversion solid state lasers.

Photon avalanche was observed for a variety of three-valent lanthanide ions such as Pr^{3+}, Nd^{3+}, Sm^{3+}, Er^{3+},Tm^{3+} as well as for Ni^{2+} (references can be found in review papers [2–4]). For some of the rare-earth ions there are several possible schemes of avalanche; of practical interest are those leading to visible emission under infrared ESA pump at a wavelength corresponding to the diode lasers.

In many cases the threshold condition for the efficiency of cross-relaxation is not easily fulfilled because it could impose active ion concentrations above the technological limit or could onset other deleterious energy transfer processes. A solution in this case could be the co-doping with a sensitizer

*Corresponding author. Fax: +40 1423 1791; e-mail: lupei@roifa.ifa.ro.

0022-2313/98/$19.00
PII S0022-2313(97)00296-2

which is able to cross-relax with the emitting ion and to transfer back the accepted excitation to the reservoir. Such a sensitized photon avalanche was recently observed in Yb-sensitized visible emission from $^3P_0$ level of Pr^{3+} in $YLiF_4$ under ESA pump in the 835 nm range from the level $^1G_4$ [5,6].

2. The physical model of sensitized avalanche

The simplified scheme of sensitized avalanche is show in Fig. 1: the significant levels of the sensitizer are the ground level (1 1) and the excited state (1 2) while for the active ion A of importance are the ground state (2 1), the reservoir (2 2) and the emitting level (2 3). The rates W_{1i} and W_{2i} characterize the intrinsic de-excitation processes (radiative and non-radiative) for these two ions in the absence of energy transfer. The parameter b is the effective branching ratio for populating the ground state (2 1) directly from the emitting level (2 3) by such intrinsic processes. For the sake of simplicity, we assume that the cross-relaxation and the back S–A transfer are characterised by the unique rates s and r, respectively, regardless of the S–A pair; for the last process this approximation is exact since at the high sensitizer concentrations usually employed in these systems, a rapid migration on the excited state of the sensitizer prior to the back transfer in the active ion could take place. This migration could also activate a three-ion cooperative excitation of the $^3P_0$ Pr^{3+} level by simultaneous transfer from two excited nearest neighbour Yb^{3+} ions (process u); the efficiency of this process could be reduced to a given extent by the inverse three-ion cross-relaxation t. ESA takes place resoantly on the strong transition (2 2) → (2 3) and weak non-resonant ground state absorption (GSA) of rate R_1 takes place in the sensitizer at the same pump wavelength.

In the case Yb-sensitized visible avalanche emission of Pr^{3+}, the levels (1 1), (1 2), (2 1), (2 2), and (2 3) correspond, respectively, to $^2F_{7/2}$ and $^2F_{5/2}$ of Yb^{3+}, $^3H_4$, $^1G_4$ and $^3P_0$ of Pr^{3+}. The $^3P_0$ level of Pr^{3+} is a very good emitter at various wavelengths from blue to near infrared; almost all these radiation processes terminate on levels below $^1G_4$ and thus the branching ratio b is close unity. The short lifetime of $^3P_0$ (of about 40–50 μs in various crystals) imposes a quite high threshold value for the efficiency of cross-relaxation process s and thus large concentrations for the sensitizer. The short lifetime of $^1G_4$ (which shows a much larger variation in different crystals, from several μs to hundreds of μs, due to the nonradiative relaxation on the nearest lower level $^3F_4$), imposes high R_2 ESA pump rates too. These can be obtained by pumping the spin allowed transition from $^1G_4$ to $^1I_6$ (in the range 830–860 nm and with a cross-section of about $0.5–2.5 \times 10^{-20}$ cm^2) from which the excitation relaxes rapidly to the near $^3P_0$ level.

3. Experimental results

The short-pulse resonantly excited room temperature luminescence of $^3P_0$ Pr^{3+} (0.2 at%) in $YLiF_4$ in the presence of Yb^{3+} (5–20 at%) shows a Yb concentration-dependent non-exponential decay due to the cross-relaxation process ($^3P_0$ Pr, $^2F_{7/2}$ Yb) → ($^1G_4$ Pr, $^2F_{5/2}$ Yb). The effective transfer rate s determined from this decay is of the order of 5×10^{-16} cm^3 s^{-1}. This pump wavelength also induces, via cross-relaxation, the emission of the $^2F_{5/2}$ level of Yb: this emission shows a characteristic rise-time determined by the decay of the donor $^3P_0$ Pr^{3+} level.

The resonant pumping of $^2F_{5/2}$ of Yb^{3+} in the presence of Pr^{3+} puts into evidence the reduction of the lifetime of this level, corresponding to an energy transfer rate r of about 1.2×10^{-16} cm^3 s^{-1}. In the beginning of the Yb^{3+} emission decay is faster, probably, due to the cooperative sensitization process u; however we could not measure yet with enough accuracy the transfer rate for the last process. From the luminescence decays in samples doped only with very small concentrations of Pr and Yb we could determine the intrinsic rates of de-excitation $W_{12} \sim 550\ s^{-1}$; $W_{22} \sim 5 \times 10^4\ s^{-1}$ and $W_{23} \sim 2.2 \times 10^4\ s^{-1}$.

Strong visible room temperature emission from blue (480 nm) to deep red (720 nm) originating from $^3P_0$ was observed in 3 nm thick Pr, Yb : $YLiF_4$ samples pumped in the 810–870 nm range by a cw Ti : sapphire laser (the maximum of emission

corresponds to about 835 nm pump). The $^3P_0$ Pr emission is accompanied by $^1G_4$ Pr and $^2F_{5/2}$ Yb emission. The pump intensity and temporal dependence of $^3P_0$ luminescence shows [5,6] features similar to those described previously for simple avalanche systems.

- at low pump intensity the emission increases steeply immediately after the onset of pumping and evolves (in a time T_p) to a stationary emission regime (plateau) whose intensity depends quadratically on the pump power.
- with increasing of pump power t_p increases to a value much larger than any lifetime from system and the shape of the rise of emission changes drastically showing a bending point; in this region of pump power the stationary emission intensity increases almost suddenly by several orders;
- by further increasing the pump power t_p decreases again and the stationary plateau shows a saturation behaviour. At high pump intensities a sharp spike (not reported for the simple avalanche systems) is observed in the initial stage of emission, followed by the plateau.

Laser emission was obtained only for the red ($^3P_0 \rightarrow {}^3F_2$) 639.5 nm transition; it also shows the early spike observed in luminescence. The luminescence emission of Yb shows features somewhat similar to those of $^3P_0$ Pr.

4. Theory

The observed features can be described by rate equation modelling: the evolutions of the populations in a luminescence experiment on the system described above are the solutions of rate equations:

$$\frac{dn_{11}}{dt} = -sn_{11}n_{23} + rn_{12}n_{21} + W_{12}n_{12} - 2tn_{11}^2n_{23} + 2un_{12}^2n_{21} - R_1n_{11},$$

$$\frac{dn_{12}}{dt} = sn_{11}n_{23} - rn_{12}n_{21} - W_{12}n_{12} + 2tn_{11}^2n_{23} - 2un_{12}^2n_{21} + R_1n_{11},$$

$$n_{11} + n_{12} = n_{10},$$

$$\frac{dn_{21}}{dt} = W_{22}n_{22} + bW_{23}n_{23} - rn_{21}n_{12} + tn_{23}n_{11}^2 - un_{12}^2n_{21},$$

$$\frac{dn_{22}}{dt} = -R_2n_{22} - W_{22}n_{22} + sn_{23}n_{11} + rn_{12}n_{21} + (1-b)W_{23}n_{23},$$

$$\frac{dn_{23}}{dt} = R_2n_{22} - W_{23}n_{23} - sn_{23}n_{11} - tn_{23}n_{11}^2 + un_{21}n_{12}^2,$$

$$n_{21} + n_{22} + n_{23} = n_{20}. \quad (1)$$

The pump rates R_1 and R_2 are determined by the pump intensity I (power density) and by the absorption cross-sections σ_1 and σ_2. While the last two parameters are constant, the pump intensity I can show large differences at the various points of the sample both due to the transverse profile in the incident beam (the modal distribution and the effect of focusing) and due to GSA and ESA along the path in the sample. Thus the system of Eq. (1) describes the populations at a given point (x,y,z) in the sample, by using the rates $R_i(x,y,z) = I(x,y,z)\sigma_i/h\nu$, where ν is the frequency of the pump quantum; for the overall response of the sample an integration over the whole pumped volume must be performed by a proper account of the spatial variation of I. In this system of rate equations we assumed that a very weak GSA takes place in a phonon tail of the $(1\,1) \rightarrow (1\,2)$ absorption ($\sigma_1 \sim 10^{-4}\,\sigma_2$). As in the case of simple avalanche processes, this system of rate equations cannot be solved analytically, except for the case of stationary regime of emission ($t \rightarrow \infty$) under a very low depletion of the sensitizer ground state and in the absence of the three-ion processes t and u: this description gives the threshold values for the pump rate R_2 and for the energy transfer processes s and r, which are functions of the various spectroscopic parameters of the system and of dopant concentrations.

Numerical modelling indicates that the condition of low depletion of state (1 1) holds only up to the avalanche threshold, and thus the threshold

values determined by the analytical solution are fairly correct. Moreover, numerical modelling enables the consideration of the three-ion processes and describes the temporal evolution of the populations regardless of the pump regime. For numerical modelling we used the spectroscopic parameters determined for the system Yb, Pr : YLF at room temperature. We also changed some of these parameters, as well as the dopant concentrations in order to put into evidence their effect upon the characteristics of the sensitized avalanche. The main conclusions from the modelling are the following:

- in the absence of the three-ion processes u and t at low R_2 pump rates (below the avalanche threshold value R_{2th}) the ground state (2 1) of the active ion is weakly depleted, mostly in the benefit of the reservoir level (2 2); the degree of depletion increases with the dopant concentrations n_{10} and n_{20}; in this regime of pump, even close to threshold, the population of the emitting level remains very weak. The populations of the levels of the active ions under cw pump evolve to stationary values; however the time t_p necessary to reach this situation is larger for n_{21} and n_{23} than for n_{22}. A similar weak depletion (dependent on concentration and with t_p close to that of n_{21}) is observed for the sensitizer ion. In this regime the t_p values increase with pump up to values of tens of milliseconds;
- In this low pump regime the presence of the three-ion processes t and u do not modify the shape of the temporal evolution of populations; however, the t_p values are reduced and the degree of depletion of the ground state (2 1) is larger.
- the three-ion processes t and u reduce the value of the avalanche threshold; thus for the sample of 0.2% Pr and 10% Yb the calculated threshold R_{2th} is in the region of $5.5–6 \times 10^4\ s^{-1}$ in agreement with the experimental data. In the absence of these processes both analytical and numerical modelling indicate a R_{2th} value of about $6.2 \times 10^4\ s^{-1}$.
- around the threshold rate R_{2th} the t_p values are maximal. The ground state of the active ion shows a stronger depletion, again in the benefit of the reservoir, at high dopant concentrations a populations inversion between these two levels can take place, although the emitting level is not very strongly populated. The depletion of the ground state of the sensitizer accentuates too, and at high concentration an inversion could take place, but at a longer time than for the active ion. The presence of the three-ion processes increases strongly the (2 2)–(2 1) inversion in the active ion but it reduces that of the sensitizer. They also change the shape of temporal evolution of the populations, especially at high dopant concentrations: the population of (2 1) is almost completely depleted, that of (2 2) is strongly increased to a maximal value (at the moment of time t_b) it then decreases slowly to a plateau. An early bump in the evolution of n_{23} is observed at t_b, followed by a slower evolution to the stationary value. These processes modify also the evolution of n_{11} and n_{12}: at t_b an almost sudden increase of n_{12} starts, evolving to the stationary state in a time similar to n_{23} (Fig. 1);
- with increasing of pump rates these processes accentuate: the t_p values decrease, the bump in evolution of n_{23} evolves to a sharp peak and the stationary value of this population increases very strongly with the pump, then follows a saturation behaviour (Fig. 2a). The stationary population of the reservoir shows a maximum value at $R_2 = (1.2–1.3)R_{2th}$, then it decreases with pump power in a depletion manner (Fig. 2b). The pump rate dependence of populations n_{22} and n_{23} are similar to those of a two-level system and the ratio (n_{23}/n_{22}) becomes linear in R_2. Physically this confirms that above R_{2th} the pump transposes the population of the reservoir (2 2) to the emitting (2 3);
- above the avalanche threshold a large but not complete depletion of the ground state of the sensitizer takes place too; from the temporal and pump dependence of the populations it is apparent that this depletion is caused by the bottleneck of the back transfer process r due to the almost complete depletion of the ground state of the active ion. This conclusion is supported by the behaviour in the presence of a laser emission between levels (2 3) and (2 1), which regenerates the population of the last of these levels: in this case the transfer r is reactivated and thus the

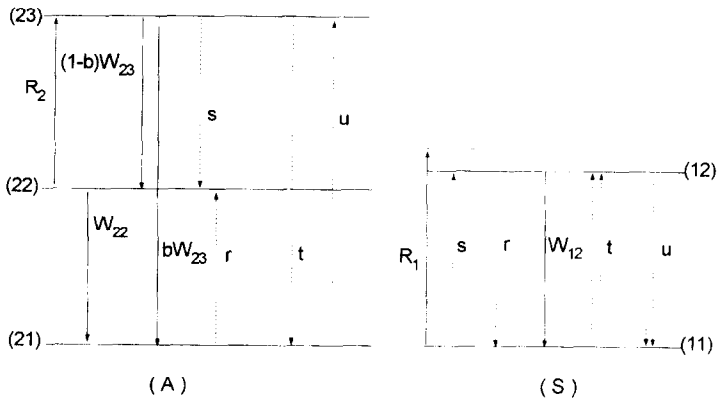

Fig. 1. The simplified scheme of sensitized photon avalanche: (A) – active ion, (S) – sensitizer.

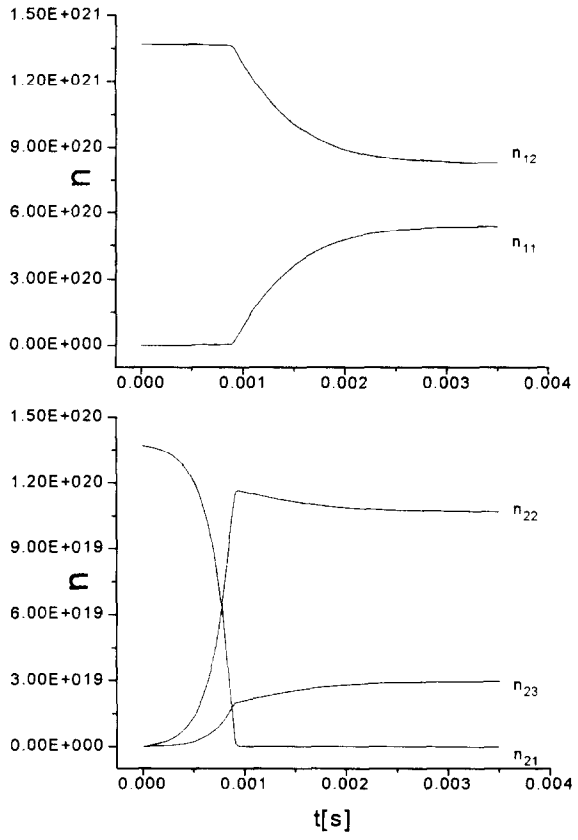

Fig. 2. Temporal evolution of populations at a pump rate R_2 immediately above threshold, for $YLiF_4$: Pr (1%), Yb (10%).

stationary population of the excited state of the sensitizer is kept to a low value.

- the early peak in the population of level (2 3) together with the reduction of R_{2th} shows that the three-ion process u has a triggering effect, similar to that induced by a small pump signal directly in the emitting level (2 3) [7]. This effect is evident in the laser emission too.

The numerical modelling at uniform pump intensities describe qualitatively several important features of the upconverted avalanche emission from level (2 3); however other experimental data are not well described and for the emission from the storage level $^1G_4$ the disagreement is even larger. Thus, while the modelling predicts that the spike induced by the three-ion cooperative sensitization process u will be placed on the rise portion of temporal evolution of emission at a time t_b smaller than t_p the measurements on Pr, Yb : $YLiF_4$ that t_p is strongly reduced toward t_b such that they can no longer be distinguished. The agreement between theory and experiment can be restored if the spatial distribution of pump (due to the mode structure, focusing and absorption) is taken into account: this shows that the various parts of the sample are pumped below, around or above the avalanche threshold and that this distribution depends on a large variety of parameters of the incident beam (the transversal distribution of intensity and the average pump power) or of the focusing system, on the characteristics of the sample (the concentrations of the dopants, the absorption cross-sections σ_1 and

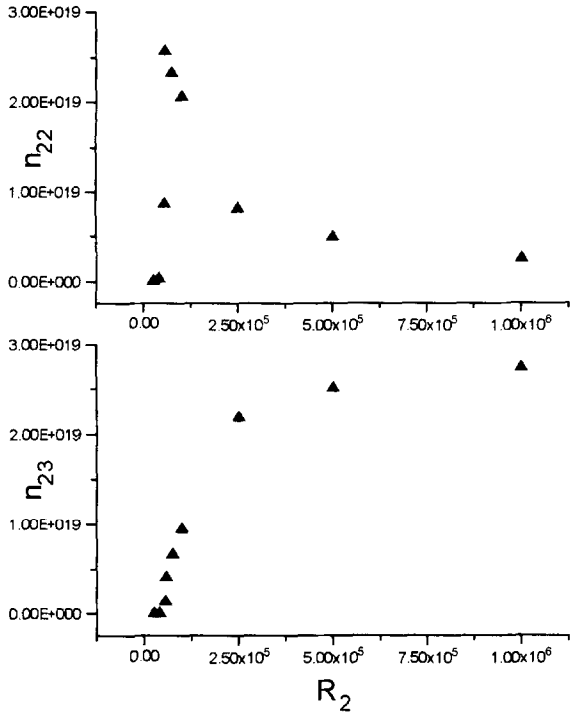

Fig. 3. Pump dependence of the stationary emission of the emitting level (a) and of the reservoir level (b) for $YLiF_4$: Pr (0.2%), Yb (10%) at uniform pump.

σ_2 at the pump wavelength) and on the geometry of the experiment (thickness of the sample or its position relative to the focal plane of lens). The overall response of the sample integrates the contributions from all the points; in case of (2 3) emission some of these global features (such as the dependence of stationary emission on pump) resemble those from the constant rate case, but for a lower rate. In case of $^1G_4$ emission, the integration smears the peak from the region of (12–1.3) R_{2th}: the emission increases slowly, then levels off at a quite low value, in good agreement with the experimental data (Fig. 3).

Strong pump distribution effects are also observed in end pumped fibre samples, but while in the case of the (thin) crystalline samples the transversal distribution seems more important, in case of fibres the pump absorption takes over.

In conclusion, the numerical modelling of the sensitized avalanche process evidences a very complex dynamics of excited state populations of both the active and sensitizer ion; these processes could determine a very efficient up-conversion of the pump radiation in the active ion, as well as a strong population inversion in the sensitizer ion. The comparison with experimental data imposes the consideration of pump distribution effects.

References

[1] J.S. Chivian, W.E. Case, D.D. Eden, Appl. Phys. Lett. 35 (1979) 124.
[2] M.F. Joubert, S. Guy, B. Jacquier, Phys. Rev. B. 48 (1993) 10031.
[3] Ph. Goldner, F. Pelle, Opt. Mat. 5 (1996) 239.
[4] M. Bouffard, J.P. Jouart, G. Mary, J. Phys. III France 6 (1996) 691.
[5] T. Sandrock, E. Heumann, G. Huber, V. Lupei, E. Osiac, B. Bejan, Int. Quantum Electronics Conf. IQEC '96, Sydney, Australia.
[6] T. Sandrock, E. Heumann, G. Huber, V. Lupei, E. Osiac, B. Bejan, CLEO-Europe/EQEC '96, Hamburg, Germany.
[7] F. Auzel, Y. Chen, J. Lumin. 65 (1995) 45.